

Error-field induced electromagnetic torques in a large aspect-ratio, low- β , weakly shaped tokamak plasma

Richard Fitzpatrick

Department of Physics, Institute for Fusion Studies, University of Texas at Austin,
Austin, Texas 78712, USA

(Received 3 October 2008; accepted 23 January 2009; published online 6 March 2009)

The toroidal electromagnetic braking torques exerted at the various internal rational surfaces of a large aspect-ratio, low- β , weakly shaped, tokamak plasma by a nonaxisymmetric error field are investigated using a semianalytic approach. It is found that there is an optimal error-field spectrum for exerting a torque at a given rational surface. This spectrum is dominated by the resonant harmonic, but also contains sideband harmonics induced by plasma toroidicity, pressure, ellipticity, and triangularity. These sidebands couple back to the resonant harmonic in such a manner as to *reduce* its amplitude. Provided that there is significant coupling to a (stable) ideal external kink mode which is close to its marginal stability boundary, the optimal error field predominately contains sideband harmonics whose poloidal mode numbers are *more positive* than the resonant mode number (which is assumed to be positive), and also tends to balloon on the *outboard* side of the plasma. © 2009 American Institute of Physics. [DOI: 10.1063/1.3081097]

I. INTRODUCTION

Tokamak plasmas are highly sensitive to static, externally generated, magnetic perturbations which break toroidal symmetry.¹⁻⁴ Such perturbations, which are conventionally termed *error fields*, are present in all tokamak experiments because of magnetic field-coil imperfections. An error field can drive *magnetic reconnection* in an otherwise tearing stable plasma, giving rise to the formation of *magnetic islands* at internal rational magnetic flux surfaces.⁵ Such islands severely degrade global energy confinement.⁶ Fortunately, the toroidal rotation which occurs naturally in all tokamak plasmas affords them some level of protection against error-field driven magnetic reconnection. To be more exact, rotation allows the development of *shielding currents* at internal rational surfaces, and these currents *suppress* the reconnection. Provided that this suppression is sufficiently strong, it is an excellent approximation to say that the response of a rotating tokamak plasma to an error field is governed by *ideal magnetohydrodynamics* (MHD). Unfortunately, the residual magnetic reconnection at the internal rational surfaces produces localized toroidal *electromagnetic torques* which *brake* the plasma rotation. Moreover, if the error-field amplitude exceeds a certain critical value—which can be as small as $\delta B/B \sim 10^{-4}$ —the torques are able to suddenly arrest the plasma rotation, and driven reconnection then proceeds without further hinderance.^{7,8} This scenario is generally known as *error-field penetration*.

The investigation of the relationship between the harmonic *spectrum* of the error-field and the *relative strengths* of the toroidal electromagnetic braking torques which develop at the various internal rational surfaces of a given tokamak plasma is central to determining which error-field harmonics need to be canceled out by external error-field correction coils, in order to prevent penetration and consequent magnetic island formation. Of course, the relationship in question is very simple in a cylindrical plasma. For in-

stance, a $m=2, n=1$ error field—where m is the poloidal mode number, and n the toroidal mode number—can only exert a torque at the 2, 1 rational surface—which is defined as the magnetic flux-surface that satisfies the resonance condition $q=m/n=2$, where q is the safety factor (i.e., the inverse of the rotational transform). Likewise, a 3, 1 error field can only exert a torque at the 3, 1 rational surface. Unfortunately, real tokamak plasmas are *toroidal*. Moreover, their magnetic flux surfaces are generally both *nonconcentric* and *noncircular*. The consequent deviations from cylindrical symmetry give rise to *coupling* between different poloidal harmonics.⁹ Thus, in a toroidal plasma, a 2, 1 error field can exert a torque at the 3, 1 rational surface, and vice versa. Indeed, recent numerical calculations have demonstrated that the relationship between the error-field spectrum and the electromagnetic torques which develop at the internal rational surfaces of a realistic small aspect-ratio, high- β , strongly shaped, tokamak plasma is *substantially different* to the corresponding relationship in a cylindrical plasma.¹⁰⁻¹²

The aim of this paper is to investigate the relationship between the error-field spectrum and the toroidal electromagnetic torques which develop at the internal rational surfaces of a large aspect-ratio, low- β , weakly shaped, tokamak plasma, i.e., a plasma in which the deviations from cylindrical geometry all remain *relatively small*. In the large aspect-ratio limit, the response of the plasma to an external error field remains sufficiently simple that it can be treated analytically. In fact, the analysis in question is very similar to that employed in Ref. 9 to investigate the tearing-mode stability of a large aspect-ratio tokamak plasma. Ultimately, the problem reduces to a set of second-order ordinary differential equations (ODEs) which are fairly straightforward to solve numerically. One advantage of this relatively simple semi-analytic approach is that extremely transparent in nature. In other words, it is very easy to see how the various noncylindrical factors, such as toroidicity, pressure, flux-surface ellip-

ticity, and flux-surface triangularity, affect the final result. The obvious disadvantage of the semianalytic approach is that it is restricted to quasicylindrical plasmas, and is, therefore, of very limited applicability to modern tokamak experiments. Nevertheless, the approach is of value for obtaining physical insight since it is far simpler than the numerical approach described in Refs. 10–12, while still being considerably more realistic than the standard cylindrical approach.⁷

In the following, all lengths are normalized to the minor radius of the plasma, a , and all magnetic field strengths to the toroidal field strength on the magnetic axis, B_0 .

II. PLASMA EQUILIBRIUM

Consider a large aspect-ratio, low- β , weakly shaped, tokamak plasma equilibrium of major radius R_0 and inverse aspect ratio $\epsilon_0 \equiv a/R_0 \ll 1$. Suppose that the safety-factor profile is

$$q(r) = \frac{q_a r^2}{1 - (1 - r^2)^\nu + \epsilon_0^2 \lambda \sin(\pi r^4)}, \quad (1)$$

where r is a flux-surface label which (to lowest order in ϵ_0) is equal to the radial distance from the magnetic axis, and $\nu = q_a/q_0$. Here, q_a and q_0 are the edge- q and the central- q values, respectively. The magnetic axis corresponds to $r=0$, and the plasma boundary to $r=1$. The toroidal plasma current profile is characterized by

$$\begin{aligned} J(r) &\equiv \frac{1}{r} \frac{d}{dr} \left(\frac{r^2}{q} \right) \\ &= \frac{2-s}{q} \\ &= \frac{2}{q_0} (1-r^2)^{\nu-1} + \epsilon_0^2 \frac{4\pi\lambda}{q_a} r^2 \cos(\pi r^4), \end{aligned} \quad (2)$$

where $s=rq'/q$ is the magnetic shear. Here, $'$ denotes d/dr . We require $\nu \geq 2$, so as to ensure that J and J' are both finite at $r=1$.

Suppose that the pressure profile, $P(r)$, takes the form

$$\epsilon_0^{-2} P(r) \equiv p(r) = \hat{\beta}_0 (1-r^2)^\alpha. \quad (3)$$

Here, $\hat{\beta}_0 = \beta_0 / \epsilon_0^2 \sim \mathcal{O}(1)$, where $\beta_0 = P_0 / (B_0^2 / \mu_0)$, and P_0 is the (un-normalized) total pressure on the magnetic axis. We require $\alpha \geq 2$, so as to ensure that p' and p'' are both finite at $r=1$.

Let us adopt a cylindrical polar coordinate system (R, ϕ, Z) aligned with the major axis of the plasma. The coordinates of the equilibrium magnetic flux surfaces are

$$R - R_0 = -r \cos \omega + \epsilon_0 (-\Delta + E \cos \omega + T \cos 2\omega) + \mathcal{O}(\epsilon_0^2), \quad (4)$$

$$Z = r \sin \omega + \epsilon_0 (E \sin \omega + T \sin 2\omega) + \mathcal{O}(\epsilon_0^2). \quad (5)$$

Here, ω is a geometric poloidal angle, centered on the magnetic axis, which is zero on the inboard midplane. Also, $\epsilon_0 \Delta(r)$ is the *Shafranov shift*, $\epsilon_0 E(r)$ is the flux-surface *ellipticity*, and $\epsilon_0 T(r)$ is the flux-surface *triangularity*. The

“straight” poloidal angle, θ , is related to the geometric angle, ω , via

$$\begin{aligned} \omega = \theta + \epsilon_0 &\left[-(\Delta' + r) \sin \theta + \frac{1}{2} \left(E' - \frac{E}{r} \right) \sin 2\theta \right. \\ &\left. + \frac{1}{3} \left(T' - 2 \frac{T}{r} \right) \sin 3\theta \right] + \mathcal{O}(\epsilon_0^2). \end{aligned} \quad (6)$$

The former angle is defined such that magnetic field-lines within flux surfaces appear as straight lines when plotted in the θ - ϕ plane.

Now, it is easily demonstrated that (to lowest order in ϵ_0) Δ , E , and T satisfy the following differential equations:

$$r^2 \Delta'' + (3-2s)r\Delta' + 2rp'q^2 - r^2 = 0, \quad (7)$$

$$r^2 E'' + (3-2s)rE' - 3E = 0, \quad (8)$$

$$r^2 T'' + (3-2s)rT' - 8T = 0. \quad (9)$$

The boundary conditions at $r=0$ are $\Delta = \Delta' = E = T = 0$. The boundary conditions at $r=1$ are $E = E_a \sim \mathcal{O}(1)$, and $T = T_a \sim \mathcal{O}(1)$, where the edge ellipticity, $\epsilon_0 E_a$, and the edge triangularity, $\epsilon_0 T_a$, are both specified. Finally, the parameter λ , appearing in Eq. (1), must be iterated until

$$\begin{aligned} \lambda = \frac{1}{4\pi} &\left(\frac{3}{2} + \Delta'^2 + 2\Delta' + E'^2 + 6EE' - 3E^2 + T'^2 \right. \\ &\left. + 16TT' - 8T^2 \right)_{r=1}, \end{aligned} \quad (10)$$

so as to ensure that the parallel plasma current at the boundary is zero to $\mathcal{O}(\epsilon_0^2)$.

III. IDEAL PLASMA RESPONSE THEORY

A. Introduction

In this section, we shall calculate the *ideal linear response* of a plasma equilibrium of the type described above to a *nonaxisymmetric error field*, with toroidal mode number n , which possesses a *dominant poloidal harmonic*.

B. Perturbed magnetic field

The perturbed magnetic field is written

$$\delta \mathbf{B} = \delta B_r \mathbf{e}_r + \delta B_\theta \mathbf{e}_\theta + \delta B_\phi \mathbf{e}_\phi, \quad (11)$$

where $\mathbf{e}_r = \nabla r / |\nabla r|$, etc. Here,

$$\delta B_r = i \sum_{m \neq 0} \frac{m}{r} \psi_m e^{i(m\theta - n\phi)} + \mathcal{O}(\epsilon_0), \quad (12)$$

$$\delta B_\theta = - \sum_{m \neq 0} \frac{d\psi_m}{dr} e^{i(m\theta - n\phi)} + \mathcal{O}(\epsilon_0), \quad (13)$$

$$\begin{aligned} \delta B_\phi = \epsilon_0 \sum_{m \neq 0} &\left\{ nZ_m + \left[J + \frac{mp'q}{r(m-nq)} \right] \psi_m \right\} e^{i(m\theta - n\phi)} \\ &+ \epsilon_0 n Z_0 e^{-in\phi} + \mathcal{O}(\epsilon_0^2). \end{aligned} \quad (14)$$

The $\psi_m(r)$ and $Z_m(r)$ satisfy

$$mr \frac{d\psi_m}{dr} = L_m^m Z_m + \sum_{j \neq 0} \left[L_m^{m+j} Z_{m+j} + \frac{(m+j)M_m^{m+j} \psi_{m+j}}{(m+j-nq)} \right], \quad (15)$$

$$(m-nq)r \frac{dZ_m}{dr} = \frac{mP_m^m \psi_m}{(m-nq)} + \sum_{j \neq 0} \left[N_m^{m+j} Z_{m+j} + \frac{(m+j)P_m^{m+j} \psi_{m+j}}{(m+j-nq)} \right]. \quad (16)$$

The various L_m^m , M_m^m , N_m^m , and P_m^m coefficients appearing in the above equations are specified in Ref. 9.

C. Ordering scheme

Assuming that ϵ_0 , β_0/ϵ_0 , $\epsilon_0 E_a$, $\epsilon_0 T_a$, $\epsilon_0 |m|$, and $\epsilon_0 n$ are all *small* compared to unity, it is consistent to adopt the following ordering scheme:

$$\psi_m = \psi_m^{(0)} + \epsilon_0^2 \psi_m^{(2)}, \quad Z_m = Z_m^{(0)} + \epsilon_0^2 Z_m^{(2)}, \quad (17)$$

$$\psi_{m+j} = \epsilon_0 \psi_{m+j}^{(1)}, \quad Z_{m+j} = \epsilon_0 Z_{m+j}^{(1)}, \quad (18)$$

$$L_m^m = L_m^{m(0)} + \epsilon_0^2 L_m^{m(2)}, \quad P_m^m = P_m^{m(0)} + \epsilon_0^2 P_m^{m(2)}, \quad (19)$$

$$L_m^{m+j} = \epsilon_0 L_m^{m+j(1)}, \quad M_m^{m+j} = \epsilon_0 M_m^{m+j(1)}, \quad (20)$$

$$N_m^{m+j} = \epsilon_0 N_m^{m+j(1)}, \quad P_m^{m+j} = \epsilon_0 P_m^{m+j(1)}, \quad (21)$$

where $j \neq 0$. Here, all quantities on the right-hand sides, other than ϵ_0 , are assumed to be $\mathcal{O}(1)$. Thus, we are searching for a solution of Eqs. (15) and (16) which is predominately an m, n harmonic, but has $\mathcal{O}(\epsilon_0)$ coupled $m+j, n$ sidebands (where $j \neq 0$). These sidebands give rise to an $\mathcal{O}(\epsilon_0^2)$ correction to the central m, n harmonic.

D. Zeroth-order solution

It follows from Eqs. (15) and (16), after a little analysis, that the zeroth-order central harmonic satisfies

$$r \frac{d}{dr} \left(r \frac{d\psi_m^{(0)}}{dr} \right) - m \left[m + \frac{qrJ'}{(m-nq)} \right] \psi_m^{(0)} = 0. \quad (22)$$

Of course, Eq. (22) is the well-known *cylindrical tearing-mode equation*. It is easily demonstrated that

$$Z_m^{(0)} = \frac{r}{m} \frac{d\psi_m^{(0)}}{dr}. \quad (23)$$

E. First-order solution

It also follows from Eqs. (15) and (16), after some analysis, that the first-order sideband harmonics satisfy

$$r \frac{d}{dr} \left(r \frac{d\psi_{m+j}^{(1)}}{dr} \right) - (m+j) \left[(m+j) + \frac{qrJ'}{(m+j-nq)} \right] \psi_{m+j}^{(1)} = mK_j \quad (24)$$

where $j \neq 0$,

$$K_j = \hat{U}_j Z_m^{(0)} + \left(Q_j \left[m + \frac{qrJ'}{(m-nq)} \right] + \hat{V}_j \right) \psi_m^{(0)}, \quad (25)$$

and

$$\hat{U}_j = U_j + \left[\frac{m(m+j-nq)}{(m-nq)} + \frac{(m+j)(m-nq)}{(m+j-nq)} \right] \hat{R}_j, \quad (26)$$

$$\hat{V}_j = V_j + \frac{(m+j-nq)\hat{O}_j}{(m-nq)} + \frac{nqsj\hat{R}_j}{(m-nq)^2} + \frac{(m+j)\hat{S}_j}{(m-nq)(m+j-nq)}. \quad (27)$$

Here,

$$Q_{\pm 1} = \Delta', \quad (28)$$

$$Q_{\pm 2} = -E', \quad (29)$$

$$Q_{\pm 3} = -T' \quad (30)$$

and

$$U_{\pm 1} = -(2-s)\Delta' - 2p'q^2 \pm 2m[(1-s)\Delta' - r], \quad (31)$$

$$U_{\pm 2} = (2-s)E' \mp \frac{1}{2}2m[(1-s)E' - 3E/r], \quad (32)$$

$$U_{\pm 3} = (2-s)T' \mp \frac{1}{3}2m[(1-s)T' - 8T/r], \quad (33)$$

plus

$$V_{\pm 1} = \mp \left[\{(1-s)(3-2s) + rs'\}\Delta' + (1-s)2p'q^2 + sr \right] + (m \pm 1)(\Delta' + r), \quad (34)$$

$$V_{\pm 2} = \pm \frac{1}{2} \left[\{(1-s)(3-2s) + rs' + 3\}E' - 3(2-s)\frac{E}{r} \right] - (m \pm 2)E', \quad (35)$$

$$V_{\pm 3} = \pm \frac{1}{3} \left[\{(1-s)(3-2s) + rs' + 8\}T' - 8(2-s)\frac{T}{r} \right] - (m \pm 3)T', \quad (36)$$

with

$$\hat{O}_{\pm 1} = \pm (rp'' + 2p's)q^2, \quad (37)$$

$$\hat{R}_{\pm 1} = \pm p'q^2, \quad (38)$$

$$\hat{S}_{\pm 1} = -(1+s)p'q^2. \quad (39)$$

Any Q_j , U_j , V_j , \hat{O}_j , \hat{R}_j , or \hat{S}_j coefficients not explicitly specified above are zero. It is easily demonstrated that

$$Z_{m+j}^{(1)} = \frac{r}{(m+j)} \frac{d\psi_{m+j}^{(1)}}{dr} - \frac{m}{(m+j)} \times \left\{ Q_j Z_m^{(0)} + \left[R_j + \frac{(m+j-nq)}{(m-nq)} \hat{R}_j \right] \psi_m^{(0)} \right\}. \quad (40)$$

F. Second-order solution

It follows from Eqs. (15) and (16), after some analysis, that the second-order correction to the central harmonic driven by the first-order sideband harmonics satisfies

$$r \frac{d}{dr} \left(r \frac{d\psi_m^{(2)}}{dr} \right) - m \left[m + \frac{qrJ'}{(m-nq)} \right] \psi_m^{(2)} = mK_0, \quad (41)$$

where

$$\begin{aligned} K_0 = & r \frac{d}{dr} \left[\left(L_0 + \frac{n^2 r^2}{m^2} \right) Z_m^{(0)} + m^{-1} \sum_{j \neq 0} (m+j) X_j \right] \\ & + \left[mP_0 + \frac{P_1}{(m-nq)} + \frac{2mrp'(1-q^2)}{(m-nq)^2} \right] \psi_m^{(0)} \\ & + \sum_{j \neq 0} (m+j) Y_j, \end{aligned} \quad (42)$$

and

$$L_0 = -\frac{3}{4}r^2 + \frac{3}{2}\Delta'^2 - \Delta + \frac{3}{2}E'^2 - \frac{3E^2}{2r^2} + \frac{3}{2}T'^2 - 4\frac{T^2}{r^2}, \quad (43)$$

$$\begin{aligned} P_0 = & \frac{7}{4}r^2 + 3r\Delta' + \frac{3}{2}\Delta'^2 + \Delta + \frac{3}{2}E'^2 - \frac{3E^2}{2r^2} + \frac{3}{2}T'^2 \\ & - 4\frac{T^2}{r^2} + \frac{1}{m^2} \left[\frac{n}{m} r^2 (2J_0 + rJ_0') - r^2 J_0'' - r^2 p'' - rp' \right], \end{aligned} \quad (44)$$

$$P_1 = -2rp'(2-s) + qr \frac{dP_2}{dr}, \quad (45)$$

$$\begin{aligned} P_2 = & \left(-\frac{r^2}{q^2} + \frac{3}{4}r^2 - \frac{3}{2}\Delta'^2 + \Delta - \frac{3}{2}E'^2 + \frac{3E^2}{2r^2} - \frac{3}{2}T'^2 \right. \\ & + 4\frac{T^2}{r^2} \Big) J_0 + \left(\frac{3}{2}r^2 + \Delta'^2 + 2r\Delta' + E'^2 + \frac{6EE'}{r} \right. \\ & \left. - 3\frac{E^2}{r^2} + T'^2 + 16\frac{TT'}{r} - 8\frac{T^2}{r^2} \right) \frac{1}{q} + J_2, \end{aligned} \quad (46)$$

with

$$X_j = Q_j Z_{m+j}^{(1)} - \left[R_j + \frac{(m-nq)}{(m+j-nq)} \hat{R}_j \right] \psi_{m+j}^{(1)}, \quad (47)$$

$$\begin{aligned} Y_j = & - \left[R_j + \frac{(m+j-nq)}{(m-nq)} \hat{R}_j \right] Z_{m+j}^{(1)} \\ & + \left[S_j + \frac{\hat{S}_j}{(m+j-nq)(m-nq)} \right] \psi_{m+j}^{(1)}, \end{aligned} \quad (48)$$

plus

$$R_{\pm 1} = \pm [(1-s)\Delta' - r], \quad (49)$$

$$R_{\pm 2} = \mp \frac{1}{2} \left[(1-s)E' - 3\frac{E}{r} \right], \quad (50)$$

$$R_{\pm 3} = \mp \frac{1}{3} \left[(1-s)T' - 8\frac{T}{r} \right], \quad (51)$$

and

$$S_{\pm 1} = \Delta' + r, \quad (52)$$

$$S_{\pm 2} = -E', \quad (53)$$

$$S_{\pm 3} = -T'. \quad (54)$$

Here, $J_0 = (2/q_0)(1-r^2)^{\nu-1}$ and $J_2 = (4\pi\lambda/q_a)r^2 \cos(\pi r^4)$ are the zeroth- and second-order components of J , respectively. Note that the $m+j=0$ harmonic does not contribute to the summations appearing in Eq. (42). Again, any R_j or S_j coefficients not explicitly specified above are zero.

G. Ideal constraints at rational surfaces

The $m+j, n$ harmonic is said to be *resonant* at $r=r_{m+j}$ provided that $q(r_{m+j}) = (m+j)/n$. If this is the case then the flux-surface $r=r_{m+j}$ is termed the $m+j, n$ *rational flux surface*. Assuming that the plasma response to the error field is essentially *ideal*, the constraints which must be satisfied at any rational surfaces lying within the plasma are

$$\psi_m^{(0)}(r_m) = \psi_{m+j}^{(1)}(r_{m+j}) = \psi_m^{(2)}(r_m) = 0, \quad (55)$$

where $j \neq 0$. Of course, these constraints ensure that there is no driven magnetic reconnection at these surfaces. In addition, they prevent Eqs. (22), (24), and (41) from becoming singular at any of the rational surfaces.

H. Boundary conditions

The boundary conditions at $r=0$ are

$$\psi_m^{(0)}(0) = \psi_{m+j}^{(1)}(0) = \psi_m^{(2)}(0) = 0. \quad (56)$$

At $r=1$, the solution is matched to a predominately m, n vacuum error field which is characterized by a *unit* zeroth order m, n normal field perturbation at $r=1$. In other words,

$$\psi_m^{(0)}(r) = \frac{r^{|m|}}{m} + \gamma_m \frac{r^{-|m|}}{m}, \quad (57)$$

for $r > 1$. Thus, the boundary condition satisfied by the zeroth-order central harmonic at $r=1$ is

$$\frac{r}{|m|} \frac{d\psi_m^{(0)}}{dr} + \psi_m^{(0)} = \frac{2}{m}. \quad (58)$$

The parameter γ_m is then determined from

$$\gamma_m = \left[-\frac{r}{|m|} \frac{d\psi_m^{(0)}}{dr} + \psi_m^{(0)} \right]_{r=1} \bigg/ \left(\frac{2}{m} \right). \quad (59)$$

The boundary conditions satisfied by the first-order sideband harmonics at $r=1$ are⁹

$$\psi_{m+j}^{(1)} = \frac{c_{m+j}}{(m+j)} + \gamma_m \frac{d_{m+j}}{(m+j)}, \quad (60)$$

where

$$c_{m+3\sigma} = \frac{(|m|+3)}{3} \left(\frac{T'}{2} - T \right)_{r=1}, \quad (61)$$

$$c_{m+2\sigma} = \frac{(|m|+2)}{2} \left(\frac{E'}{2} - \frac{E}{2} \right)_{r=1}, \quad (62)$$

$$c_{m+\sigma} = -(|m|+1) \left(-\frac{1}{4|m|} \frac{1-|m|}{1+|m|} + \frac{\Delta'}{2} \right)_{r=1}, \quad (63)$$

$$c_{m-\sigma} = (|m|-1) \left(-\frac{1-2|m|}{4|m|} + \frac{\Delta'}{2} + \Delta \right)_{r=1}, \quad (64)$$

$$c_{m-2\sigma} = -\frac{(|m|-2)}{2} \left(\frac{E'}{2} + \frac{3E}{2} \right)_{r=1}, \quad (65)$$

$$c_{m-3\sigma} = -\frac{(|m|-3)}{3} \left(\frac{T'}{2} + 2T \right)_{r=1}, \quad (66)$$

and

$$d_{m+3\sigma} = \frac{(|m|+3)}{3} \left(\frac{T'}{2} + 2T \right)_{r=1}, \quad (67)$$

$$d_{m+2\sigma} = \frac{(|m|+2)}{2} \left(\frac{E'}{2} + \frac{3E}{2} \right)_{r=1}, \quad (68)$$

$$d_{m+\sigma} = -(|m|+1) \left(\frac{1+2|m|}{4|m|} + \frac{\Delta'}{2} + \Delta \right)_{r=1}, \quad (69)$$

$$d_{m-\sigma} = (|m|-1) \left(\frac{1}{4|m|} \frac{1+|m|}{1-|m|} + \frac{\Delta'}{2} \right)_{r=1}, \quad (70)$$

$$d_{m-2\sigma} = -\frac{(|m|-2)}{2} \left(\frac{E'}{2} - \frac{E}{2} \right)_{r=1}, \quad (71)$$

$$d_{m-3\sigma} = -\frac{(|m|-3)}{3} \left(\frac{T'}{2} - T \right)_{r=1}. \quad (72)$$

Here, $\sigma \equiv \text{sgn}(m)$.

Finally, the boundary condition satisfied by the second-order correction to the central harmonic at $r=1$ is⁹

$$\psi_m^{(2)} = \frac{1}{m} [(G_0 + \gamma_m G_3) + |m| G_1 (1 - \gamma_m) + m^2 G_2 (1 + \gamma_m)], \quad (73)$$

where

$$G_0 = \left[\frac{(|m|+2)n^2 - |m|^2/4}{4(|m|+1)|m|} \right], \quad (74)$$

$$G_1 = \left(\frac{1}{4}\Delta' + \frac{1}{2}\Delta\Delta' + \frac{1}{4}\Delta + \frac{1}{2}EE' + \frac{1}{2}TT' \right)_{r=1}, \quad (75)$$

$$G_2 = \left[-\frac{1}{4}\Delta' + \frac{1}{4}\Delta^2 - \frac{1}{4}(\Delta' + \Delta)^2 + \frac{1}{4}E^2 - \frac{1}{16}(E' + E)^2 + \frac{1}{4}T^2 - \frac{1}{36}(T' + T)^2 \right]_{r=1}, \quad (76)$$

$$G_3 = - \left[\frac{(|m|-2)n^2 + |m|^2/4}{4(|m|-1)|m|} \right]. \quad (77)$$

For the special case $|m|=1$, G_3 takes the value

$$G_3 = - \left[\frac{n^2}{4} - \frac{1}{8} + \left(\frac{n^2}{2} - \frac{1}{8} \right) \ln \left(\frac{\zeta}{8} \right) \right], \quad (78)$$

where

$$\zeta = \exp \left(\sum_{i=1,n} \frac{2}{2i-1} \right). \quad (79)$$

IV. ELECTROMAGNETIC TORQUES

In this section, we shall calculate the toroidal electromagnetic torques exerted at the internal rational flux surfaces of a plasma equilibrium of the type described in Sec. II by a *general* nonaxisymmetric error field of toroidal mode number n . Note that such an error field can always be written as a linear superposition of error fields with the same toroidal mode number but various different dominant poloidal mode numbers. In other words, a general error field can be built up out of a combination of the special error fields described in Sec. III.

We can conveniently characterize the vacuum error field normal to the plasma boundary in terms of a complex vector, \mathbf{b} , whose elements, b_m , are obtained from

$$b_r^{\text{vac}}(1, \theta, \phi) = \sum_{m \neq 0} b_m e^{i(m\theta - n\phi)}. \quad (80)$$

However, according to the analysis in Sec. III,

$$b_m = \sum_{m' \neq 0} C_{m,m'} \alpha_{m'}, \quad (81)$$

where the α_m are a set of arbitrary complex coefficients, and

$$C_{m+3\sigma,m} = \epsilon_0 \frac{(|m|+3)}{3} \left(\frac{T'}{2} - T \right)_{r=1}, \quad (82)$$

$$C_{m+2\sigma,m} = \epsilon_0 \frac{(|m|+2)}{2} \left(\frac{E'}{2} - \frac{E}{2} \right)_{r=1}, \quad (83)$$

$$C_{m+\sigma,m} = -\epsilon_0 (|m|+1) \left(-\frac{1}{4|m|} \frac{1-|m|}{1+|m|} + \frac{\Delta'}{2} \right)_{r=1}, \quad (84)$$

$$C_{m,m} = 1 + \epsilon_0^2 (G_0 + |m| G_1 + m^2 G_2), \quad (85)$$

$$C_{m-\sigma,m} = \epsilon_0 (|m|-1) \left(-\frac{1-2|m|}{4|m|} + \frac{\Delta'}{2} + \Delta \right)_{r=1}, \quad (86)$$

$$C_{m-2\sigma,m} = -\epsilon_0 \frac{(|m|-2)}{2} \left(\frac{E'}{2} + \frac{3E}{2} \right)_{r=1}, \quad (87)$$

$$C_{m-3\sigma,m} = -\epsilon_0 \frac{(|m|-3)}{3} \left(\frac{T'}{2} + 2T \right)_{r=1}. \quad (88)$$

All other elements of the C -matrix are zero. Observe that the diagonal elements of the C -matrix are $\mathcal{O}(1)$, with $\mathcal{O}(\epsilon_0^2)$ cor-

rections, whereas the off-diagonal elements are $\mathcal{O}(\epsilon_0)$.

Suppose that the m, n harmonic is resonant at $r=r_m$. We can write

$$\mathcal{J}_m \equiv \left[r \frac{d\psi_m}{dr} \right]_{r_{m-}}^{r_{m+}} = \sum_{m' \neq 0} F_{m,m'} \alpha_{m'}, \quad (89)$$

where

$$F_{m,m'} = \left[r \frac{d\hat{\psi}_{m,m'}}{dr} \right]_{r_{m-}}^{r_{m+}}. \quad (90)$$

Here, the $\hat{\psi}_{m,m'}(r)$ are $\psi_m(r)$ functions of the type calculated in Sec. III for a central poloidal harmonic m' . In other words, $\hat{\psi}_{m,m} = \psi_m^{(0)} + \epsilon_0^2 \psi_m^{(2)}$ and $\hat{\psi}_{m,m+j} = \epsilon_0 \psi_{m+j}^{(1)}$ for $j \neq 0$. Moreover, $\psi_m^{(0)}$ is the solution of Eq. (22), subject to constraint (55), and the boundary conditions (56) and (58). Furthermore, $\psi_{m+j}^{(1)}$ is the solution of Eq. (24), subject to constraint (55), and the boundary conditions (56) and (60). Finally, $\psi_m^{(2)}$ is the solution of Eq. (41), subject to constraint (55), and the boundary conditions (56) and (73). Clearly, the diagonal elements of the F -matrix are $\mathcal{O}(1)$, with $\mathcal{O}(\epsilon_0^2)$ corrections, whereas the off-diagonal elements are $\mathcal{O}(\epsilon_0)$.

Asymptotic matching at the m, n rational surface yields¹³

$$\Delta_m \Psi_m = \Delta'_m \Psi_m + \mathcal{J}_m, \quad (91)$$

where Δ_m is the (generally complex) *layer response function*, Δ'_m is the (real) *tearing stability index*, and Ψ_m is the *reconnected magnetic flux*. Both Δ_m and Δ'_m are *independent* of the error field. For a tearing stable plasma, Δ'_m is negative and generally $\mathcal{O}(1)$. Now, the magnitude of the shielding current flowing at the rational surface is proportional to $|\Delta_m|$. In the absence of shielding, the error field drives substantial magnetic reconnection. Indeed, the reconnected magnetic flux in this case is

$$\Psi_{m \text{ full}} = \frac{\mathcal{J}_m}{-\Delta'_m}. \quad (92)$$

However, *toroidal plasma rotation* produces strong shielding at the rational surface, i.e., $|\Delta_m| \gg 1$. In this situation, magnetic reconnection is largely *suppressed* so that $|\Psi_m| \ll |\Psi_{m \text{ full}}|$. In other words, in the presence of strong rotational shielding, the plasma response at the rational surface is essentially *ideal*, i.e., similar to that obtained in the limit $|\Delta_m| \rightarrow \infty$. Nevertheless, the small nonideal component of the plasma response is important since it allows the error field to exert an electromagnetic torque at the surface.

The toroidal electromagnetic torque exerted at the m, n rational surface is given by⁹

$$T_m = \frac{n}{2r_m} |\mathcal{J}_m|^2 \frac{\text{Im}(\Delta_m)}{|\Delta_m - \Delta'_m|^2}. \quad (93)$$

In the strong shielding limit, this reduces to

$$T_m \approx -\frac{n}{2r_m} |\mathcal{J}_m|^2 \text{Im}(1/\Delta_m). \quad (94)$$

Thus, in an *almost ideal* plasma (i.e., $\infty > |\Delta_m| \gg 1$) the error field can exert a relatively small electromagnetic torque at

the m, n rational surface. Moreover, all of the dependence of this torque on the error field is contained within the $|\mathcal{J}_m|^2$ factor. Hence, we just need to understand the relationship between this factor and the error-field spectrum. Note that $|\mathcal{J}_m|^2$ is fully determined by the ideal-MHD response theory discussed in Sec. III, and is completely independent of any nonideal layer physics which holds in the immediate vicinity of the m, n rational surface. It follows that the optimal error-field spectrum for exerting a torque at the m, n rational surface is likewise independent of layer physics.

According to Eqs. (81) and (89),

$$\mathcal{J}_m = \mathbf{h}_m \cdot \mathbf{b}, \quad (95)$$

where the elements of the \mathbf{h}_m vector are given by

$$(\mathbf{h}_m)_{m'} \equiv H_{m,m'} = \sum_{k \neq 0} F_{m,k} C_{k,m'}^{-1}. \quad (96)$$

However, to be consistent with our ordering scheme, it is only necessary to calculate the diagonal elements of the H -matrix to $\mathcal{O}(\epsilon_0^2)$, and the off-diagonal elements to $\mathcal{O}(\epsilon_0)$. It follows that

$$H_{m,m} \approx F_{m,m} \left(2 - C_{m,m} + \sum_{k \neq m} C_{m,k} C_{k,m} \right) - \sum_{k \neq m} F_{m,k} C_{k,m}, \quad (97)$$

and

$$H_{m,m'} \approx -F_{m,m} C_{m,m'} + F_{m,m'} \quad (98)$$

for $m \neq m'$.

Now, the *magnitude* of the error-field vector, \mathbf{b} , specifies the *root-mean-square amplitude* of the vacuum error field normal to the plasma boundary, whereas its *direction* determines the error-field *spectrum*. Thus, it is clear from Eq. (95) that at fixed rms error-field amplitude, the error-field spectrum which *maximizes* the electromagnetic torque exerted at the m, n rational surface is such that the \mathbf{b} vector is *parallel* to the \mathbf{h}_m vector. In this case,

$$|\mathcal{J}_m|^2 = |\mathbf{h}_m|^2 |\mathbf{b}|^2. \quad (99)$$

So, at fixed rms error-field amplitude, the electromagnetic torque is proportional to the *magnitude squared* of the \mathbf{h}_m vector. In other words, the *direction* of the \mathbf{h}_m vector specifies the *optimal error-field spectrum* for exerting a torque at the m, n rational surface, whereas the *magnitude* of this vector characterizes the *maximum torque* which can be exerted at the rational surface by an error field of fixed rms amplitude (assuming strong shielding).

V. EXAMPLE CALCULATION

Consider an example plasma equilibrium characterized by $q_0=1.5$, $q_a=3.9$, and $\alpha=2.0$. The associated safety-factor profile is shown in Fig. 1. Suppose that this equilibrium interacts with an $n=1$ error field. It follows that there are two rational flux-surfaces inside the plasma, i.e., the 2, 1 surface at which $q=2$, and the 3, 1 surface at which $q=3$. The former surface lies at $r=0.580$, and the latter at $r=0.865$ (see Fig. 1).

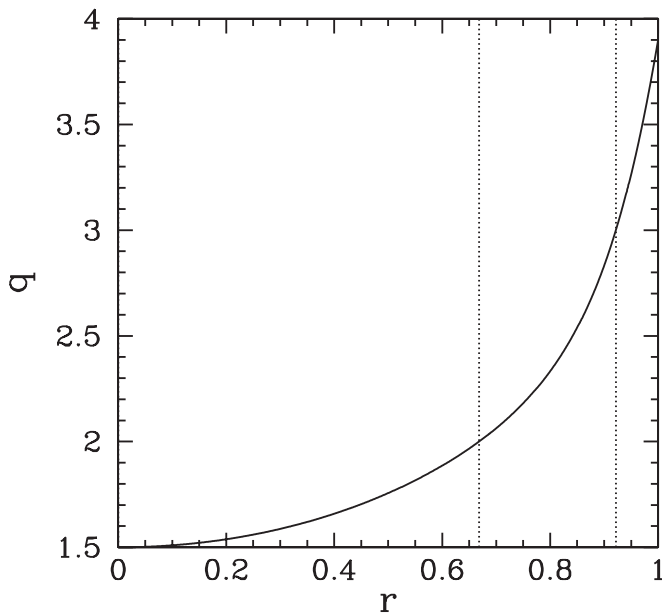


FIG. 1. Safety-factor profile for a plasma equilibrium characterized by $q_0 = 1.5$ and $q_a = 3.9$. The positions of the $q=2$ and $q=3$ surfaces are indicated by vertical dotted lines.

The \mathbf{h}_2 vector, which characterizes the toroidal electromagnetic braking torque exerted by an $n=1$ error field at the $q=2$ surface, is calculated to have the following non-negligible components:

$$(h_2)_{-1} = -0.371T_a, \quad (100)$$

$$(h_2)_1 = 0.322\epsilon_0 + 1.95\beta_0/\epsilon_0, \quad (101)$$

$$(h_2)_2 = 0.240 - 0.183\epsilon_0^2 - 130.3(\beta_0/\epsilon_0)^2 - 18.0\beta_0 - 3.70E_a^2 - 0.085T_a^2, \quad (102)$$

$$(h_2)_3 = 0.045\epsilon_0 - 0.921\beta_0/\epsilon_0, \quad (103)$$

$$(h_2)_4 = 2.82E_a, \quad (104)$$

$$(h_2)_5 = 1.40T_a. \quad (105)$$

Recall that the optimal vacuum error field for exerting a torque at the $q=2$ surface has the *same spectrum* as the \mathbf{h}_2 vector. We conclude that, in a large aspect-ratio, low- β , weakly shaped, tokamak plasma equilibrium (i.e., an equilibrium in which ϵ_0 , β_0/ϵ_0 , $\epsilon_0 E_a$, and $\epsilon_0 T_a$ are all much less than unity), the optimal error field is dominated by the resonant 2, 1 harmonic, but also possesses smaller sideband harmonics driven by plasma toroidicity, pressure, ellipticity, and triangularity. Moreover, these sidebands couple back to the resonant harmonic in such a way as to *reduce* its magnitude.

There are two interesting metrics which can be applied to a given \mathbf{h}_m vector. The first metric,

$$S_m = \sum_{m' > m} \frac{|H_{m,m'}|}{H_{m,m}} - \sum_{m' < m} \frac{|H_{m,m'}|}{H_{m,m}}, \quad (106)$$

measures the extent to which the optimal error field predominately contains sideband harmonics with poloidal mode

numbers which are *more positive*, rather than *more negative*, than the resonant mode number (which is assumed to be positive). Thus, if $S_m > 0$ then the optimal error field predominately contains sideband harmonics whose poloidal mode numbers are more positive than the resonant mode number, and vice versa. The second metric,

$$B_m = \left| \frac{\sum_{m'} H_{m,m'} (-1)^{(m'-m)}}{\sum_{m'} H_{m,m'}} \right| - 1, \quad (107)$$

measures the extent to which the amplitude of the optimal error field on the *outboard* midplane ($\theta = \pi$) exceeds that on the *inboard* midplane ($\theta = 0$). Thus, if $B_m > 0$ then the optimal error field has a higher amplitude on the outboard midplane, and vice versa.

For the previously specified \mathbf{h}_2 vector, we find that

$$S_2 = -1.16\epsilon_0 - 4.30\beta_0/\epsilon_0 + 11.8E_a + 4.30T_a, \quad (108)$$

$$B_2 = -3.07\epsilon_0 - 8.60\beta_0/\epsilon_0 - 8.59T_a. \quad (109)$$

It follows that toroidicity and pressure favor an optimal error field which predominately contains sideband harmonics with poloidal mode numbers which are *more negative* than the resonant mode number, whereas flux-surface shaping favor an error field which predominately contains sideband harmonics with mode numbers which are *more positive* than the resonant mode number. Moreover, toroidicity, pressure, and flux-surface shaping all tend to make the optimal error-field balloon on the *inboard* side of the plasma.

The \mathbf{h}_3 vector, which characterizes the toroidal electromagnetic braking torque exerted by an $n=1$ error field at the $q=3$ surface, is calculated to have the following non-negligible components:

$$(h_3)_1 = -1.51E_a \quad (110)$$

$$(h_3)_2 = 1.57\epsilon_0 + 9.82\beta_0/\epsilon_0, \quad (111)$$

$$(h_3)_3 = 1.03 - 4.28\epsilon_0^2 - 591.2(\beta_0/\epsilon_0)^2 - 103.1\beta_0 - 8.82E_a^2 - 1.16T_a^2, \quad (112)$$

$$(h_3)_4 = -1.86\epsilon_0 - 24.2\beta_0/\epsilon_0, \quad (113)$$

$$(h_3)_5 = 1.16E_a, \quad (114)$$

$$(h_3)_6 = 5.87T_a. \quad (115)$$

Note that, as before, the optimal error field is dominated by the resonant harmonic, but contains sideband harmonics which couple back to the resonant harmonic in such a way as to *reduce* its magnitude.

For the case of the \mathbf{h}_3 vector, our two metrics take the form

$$S_3 = 0.286\epsilon_0 + 13.9\beta_0/\epsilon_0 - 0.333E_a + 5.68T_a, \quad (116)$$

$$B_3 = 0.572\epsilon_0 + 27.8\beta_0/\epsilon_0 - 11.4T_a. \quad (117)$$

We conclude that toroidicity and pressure now favor an optimal error field which predominately contains sideband harmonics with *more positive* poloidal mode numbers than the

resonant mode number, and also tend to make the optimal error-field balloon on the *outboard* side of the plasma.

It turns out that the 4, 1 ideal external kink mode is fairly close to marginal stability (but still stable) for the chosen plasma equilibrium (since the $q=4$ surface lies just outside the plasma, and the central- q value is relatively high). For the case of the \mathbf{h}_2 vector, coupling between the error field and the 4, 1 mode is controlled by plasma *ellipticity*. On the other hand, for the case of the \mathbf{h}_3 vector, coupling to the 4, 1 mode is controlled by *toroidicity* and *pressure*. Equations (108), (109), (116), and (117) strongly suggest that coupling to a (stable) ideal external kink mode which is close to marginal stability causes the optimal error field for exerting a torque at a given internal rational surface to predominately contain sideband harmonics whose poloidal mode numbers are *more positive* than the resonant mode number, and to balloon on the *outboard* side of the plasma. [Note that the latter effect is not evident in Eq. (109) because flux-surface ellipticity makes no contribution to the in-out asymmetry of the optimal error field.] Conversely, in the absence of coupling to an ideal external kink mode which is close to marginal stability, the optimal error field predominately contains sideband harmonics whose poloidal mode numbers are *more negative* than the resonant mode number, and also tends to balloon on the *inboard* side of the plasma. This can be seen more explicitly by lowering the central q -value, which has the effect of stabilizing the 4, 1 external kink mode.

VI. SUMMARY

We have investigated the toroidal electromagnetic braking torques exerted at the various internal rational surfaces of a large aspect-ratio, low- β , weakly shaped, tokamak plasma equilibrium by a nonaxisymmetric error field. In the large aspect-ratio limit, the problem remains sufficiently simple that it is amenable to analysis, and eventually reduces to a set of second-order ODEs, Eqs. (22), (24), and (41), subject to constraint (55), and the boundary conditions (56), (58), (60), and (73). It is a straightforward task to obtain numerical solutions to these equations. In Sec. IV, it is shown how such solutions can be used to calculate the optimal error-field spectrum for exerting a torque at a given rational surface within the plasma. We find that the optimal spectrum is *entirely determined* by *ideal-MHD* plasma response theory, and is *independent* of any nonideal layer physics which holds in the immediate vicinity of the internal rational surfaces (assuming that driven magnetic reconnection is strongly shielded by plasma rotation).

The optimal error-field spectrum for exerting a torque at a given rational surface is found to be dominated by the resonant harmonic, but also contains sideband harmonics induced by plasma toroidicity, pressure, ellipticity, and triangularity. Moreover, these sidebands couple back to the resonant harmonic in such a manner as to reduce its amplitude. Unfortunately, our fundamental large aspect-ratio ordering precludes us from obtaining an optimal error-field spectrum

in which the resonant harmonic is not dominant. Hence, we cannot directly compare our results with the numerical calculations described in Refs. 10–12, which employ realistic small aspect-ratios, and which find optimal error-field spectra which are not dominated by the resonant harmonic.

Generally speaking, if there is significant coupling to a (stable) ideal external kink mode which is close to its marginal stability boundary then we find that the optimal error field predominately contains side-band harmonics whose poloidal mode numbers are more positive than the resonant mode number (which is assumed to be positive), and also tends to balloon on the outboard side of the plasma. On the other hand, if there is no such coupling then the optimum error field predominately contains sideband harmonics whose poloidal mode numbers are more negative than the resonant mode number, and also tends to balloon on the inboard side of the plasma.

The semianalytic approach presented in this paper is obviously of very limited applicability to modern tokamak experiments because it can only deal with quasicylindrical plasmas. Nevertheless, it is of value for obtaining physical insight, since it is comparatively simple, and also allows us to see, in a very clear manner, how the various noncylindrical effects in a quasicylindrical plasma—such as toroidicity, pressure, flux-surface ellipticity, and flux-surface triangularity—affect the optimal error-field spectrum for exerting a torque at a given rational surface within the plasma. Our semianalytic approach also represents a significant improvement over the standard cylindrical approach which has been used previously, with some success, to investigate the electromagnetic torques exerted on tokamak plasmas by error fields.^{7,8}

ACKNOWLEDGMENTS

This research was funded by the U.S. Department of Energy under Contract No. DE-FG05-96ER-54346.

¹J. T. Scoville, R. J. La Haye, A. G. Kellman, T. H. Osborne, R. D. Stambaugh, E. J. Strait, and T. S. Taylor, *Nucl. Fusion* **31**, 875 (1991).

²T. C. Hender, R. Fitzpatrick, A. W. Morris, P. G. Carolan, R. D. Durst, T. Edlington, J. Ferreira, S. J. Fielding, P. S. Haynes, J. Hugill, I. J. Jenkins, R. J. La Haye, B. J. Parham, D. C. Robinson, T. N. Todd, M. Valovic, and G. Vayakis, *Nucl. Fusion* **32**, 2091 (1992).

³G. M. Fishpool and P. S. Haynes, *Nucl. Fusion* **34**, 109 (1994).

⁴S. M. Wolfe, I. H. Hutchinson, R. S. Granetz, J. Rice, A. Hubbard, A. Lynn, P. Phillips, T. C. Hender, and D. F. Howell, *Phys. Plasmas* **12**, 056110 (2005).

⁵A. H. Boozer, *Rev. Mod. Phys.* **76**, 1071 (2005).

⁶Z. Chang and J. D. Callen, *Nucl. Fusion* **30**, 219 (1990).

⁷R. Fitzpatrick, *Nucl. Fusion* **33**, 1049 (1993).

⁸R. Fitzpatrick, *Phys. Plasmas* **5**, 3325 (1998).

⁹R. Fitzpatrick, R. J. Hastie, T. J. Martin, and C. M. Roach, *Nucl. Fusion* **33**, 1533 (1993).

¹⁰J.-K. Park, A. H. Boozer, and A. H. Glasser, *Phys. Plasmas* **14**, 052110 (2007).

¹¹J.-K. Park, M. J. Schaffer, J. E. Menard, and A. H. Boozer, *Phys. Rev. Lett.* **99**, 195003 (2007).

¹²J.-K. Park, A. H. Boozer, J. E. Menard, and M. J. Schaffer, *Nucl. Fusion* **48**, 045006 (2008).

¹³H. P. Furth, J. Killeen, and M. N. Rosenbluth, *Phys. Fluids* **6**, 459 (1963).